VOL. 10, NO 19, OCTOBER, 2015 ISSN 1819-6608
ARPN Journal of Engineering and Applied Sciences

www.arpnjournals.com

DEFECTED GROUND STRUCTURE FOR BEAM STEERING ARRAY ANTENNA APPLICATIONS

K. S. Ahmad[1, 2], S. A. Hamzah F.[1] and F. C. Seman
[1]Wireless and Radio Science Center, University Tun Hussein Onn Malaysia (UTHM), Batu Pahat, Johor, Malaysia
[2]Department of Electronic, Technical Institute Mosul, Foundation of Technical Education, Iraq
E-Mail: fauziahs@uthm.edu.my

ABSTRACT

Incorporation of Defected Ground Structure (DGS) into the Microstrip Phased Array Antenna (PAA) provides desirable changes to the direction of the main beam. In this paper, investigation on the development of 2 x 1 rectangular patches which operates at 9 GHz is presented. The two rectangular patches are separated at 0.258λ and the microstrip line is feeding to the center of the patches to provide impedance matching. Then, an orthogonal-I-shaped DGS is inserted in between the two patches at the ground plane. It is found that by changing the dimension of the DGS, the main lobe of the PAA increases from 39° to 137°, however, the directivity of the arrays maintains about 6 dBi. This demonstrates the potential of employing DGS to steer the main beam of PAA instead of using additional phase shifter which is bulky and more complicated to connect to the antenna's feeding line.

Keywords: phase array antenna, beam steering, defected ground structure (DGS) modification.

INTRODUCTION

The need for a low-cost and powerful PAA yet simple to operate at microwave and millimeter wave frequencies has increased over the recent years. A steerable antenna with tunable phase shifter continues to be a popular choice of radio operator to provide such systems. However, this additional device makes the structure more complicated and bulky. Therefore, it creates new challenges for antenna designer to find an alternative device that able to provide similar features hence maintains the similar performance. One of it is an employment of DGS at the RF front-ends circuit to support different beam angle. This leads to a new perspective on the development of beam steering antenna array that able to steer the beam angle.

The concept of PAA was proposed by a Lincoln Laboratory in 1958 (Bin, 2011). The PAA are subsequently known for their capability to steer the beam pattern electronically with high effectiveness. In principle, the beam steering system is the most important subsystem for the PAA. To achieve the eligible design parameters such as narrow beam width and low side-lobe levels, an excellent beam steering system is necessary for controlling the phase shift of antenna elements (Bin, 2011). The common technique to achieve a beam-switching is either electronically to form radiators into an array or mechanically with the controlled motor. By controlling the phase of the surface current on the radiator, the radiation pattern can be steered (Haitao, 2012).

Microstrip array antennas are widely used because of their attractive features such as ease to fabricate, low profile, small size, light weight, and low cost (Habashi, 2012). They are used frequently in the phased array antenna such as for pattern beamforming, smart antenna and electronic scanning radars (Hajilou, 2012).

Employment of DGS in PAA system was previously shown able to reduce the mutual coupling as well as optimizing the radiation pattern (Hajilou, 2012), (Ismaiel, 2014), (Xiao, 2011), (Jin, 2012), (Ahmed, 2012), for harmonic frequencies suppression (Chaozhu, 2014), circuit size reduction (Vikash, 2013), and mitigation on the back and side – lobe (Xiao, 2011), (Alias, 2013). Some of the phase shifters have been proposed based on the DGS circuit, which is originally used in filter, coupler, and oscillator designs (Can, 2014). DGS disturbs the current distribution direction and commonly it is positioned on the ground plane. This disturbance changes the electrical characteristic of the transmission line by manipulating capacitance and inductance in the representation of equivalent circuit in order to obtain slow-wave effect and band-stop property (Vikash, 2013).

Beam steering method and phased array antennas

PAA system consists of an array elements, feeding network, phase shifter in order to provide the necessary phase difference between these elements for the necessary steering of the beam in a desired direction (Armenta, 2012). Figure-1 shows a geometry of *N* element linear array antenna, where each element is separated by *d* over a straight line and feeding with the same agitation amplitude and phase difference (Balanis, 2005), (Volakis, 2007), (Haupt, 2010). This steering of the beam is due to resultant sum/cancellation of electric field vectors of each element which results in the constructive/destructive interference (Shafaat, 2012).

ANTENNA DESIGN

Planar array antenna design and DGS

The proposed configuration in Figure-2 is used to demonstrate the beam steering capability in PAA. The structure includes 2×1 rectangular element patch array, 50Ω microstrip fed line. Table-1 shows the dimension of the rectangular patch that is simulated on FR-4 board with a relative permittivity of 4.4, loss tangent of 0.02 and the

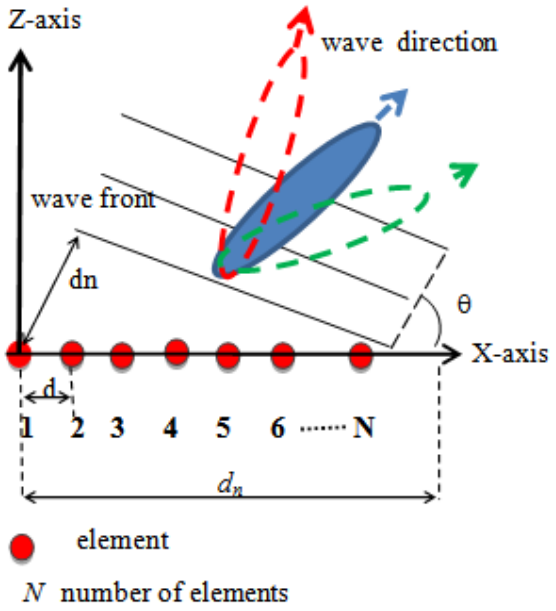

Figure-1. Geometry of *N* element linear array antenna positioned along the x-axis.

thickness of 1.0 mm. Both elements have an equal dimension of width, 14 mm and length, 15 mm and each is separated by 8.5 mm spacing. In this study, the simulations work have been carried by using the frequency domain solver in CST MWS with open (add space) boundary conditions. The SMA-port excitation is used in this simulation.

Table-1. Design specification of rectangular patch.

Parameters	Parameters Dimensions
Substrate Type	FR4, loss tangent of 0.02
Dielectric Constant	4.4
Substrate Height	1mm
Center Frequency	9.08 GHz
Patch Thickness	0.070 mm

Later, an orthogonal-I-shaped of DGS with the size of 9 x 6.25 mm is inserted on the ground plane. The open (add space) boundaries are chosen at the top and the bottom sides for the z-direction with distance to the reference plane of -7h or (-7.4947 mm). For the x-direction and y-direction, the electric boundary condition $E_{tan}=0$ and magnetic boundary condition $H_{tan}=0$. The waveguide port excitation is used in this simulation. The distance of the DGS and the edge of the radiation element are optimized through the parametric study to 1.125 mm. With proper position and dimension, this slot can exhibit a beam steering (Can, 2013), (Chirag, 2014) with slightly small change in frequency shift due to slow-wave effects (Ahmed, 2012). Figure-3 shows the schematic diagram of an optimum dimension of the orthogonal I-shaped DGS. The structure is inserted on the ground plane between two radiated elements. The dimension of the DGS is the key parameter for changing the resonant frequency (Shikha, 2013), and therefore in this paper, the impact of beam steering capability is observed by varying *a* at 5 different values.

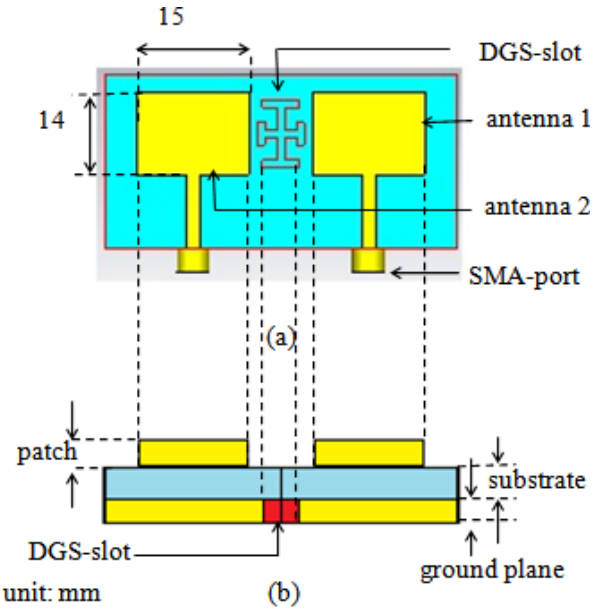

Figure-2. The antenna array structure with orthogonal–I-shaped DGS (a) top view geometry (b) side view.

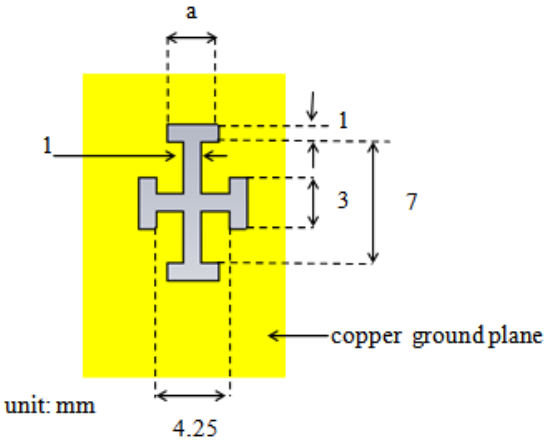

Figure-3. Schematic of orthogonal-I-shaped DGS.

Simulated results

Figure-4 shows planar arrays resonates at 9.08 GHz with a return loss of -24.60 dB. Without the DGS slot, the ground plane reflects the incoming signal at 180° with negligible loss as illustrated in Figure-5. The dimension *a* is varying at 5 different values which are 1 mm, 3 mm, 5.0 mm, 5.5 mm and 7 mm while keeping the other values constant. Figure-5 (a) demonstrates the resonant frequency of the DGS reduces from 11.22 GHz to 8.25 GHz when *a* increases from 1 mm to 7 mm. The resonance of the DGS is inversely proportional to the size of *a* because it enlarges the effective series inductance of the line. When *a* = 5 mm, the DGS's resonates at 9.1 GHz which is closed to the operating frequency of the rectangular patches as described previously in Figure-4.

In reflection phase perspective, Figure-5(b) shows, when *a* = 1 mm, the reflection phase about the DGS resonant frequency (11.2 GHz) increases from 92° to 267°

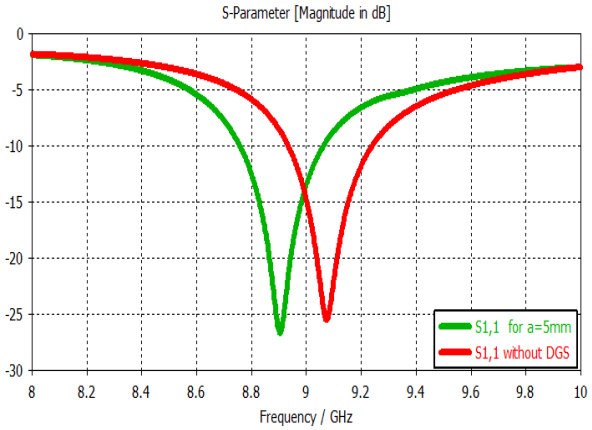

Figure-4. S_{11} response for array antenna with and without DGS.

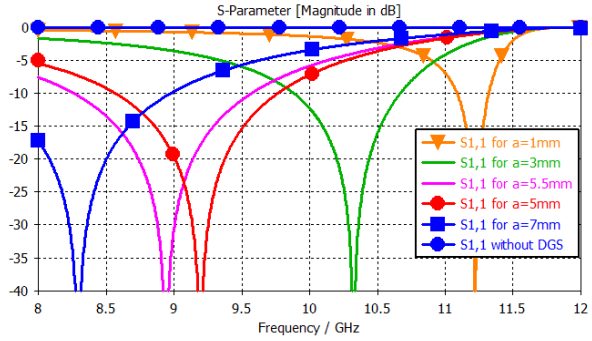

(a)

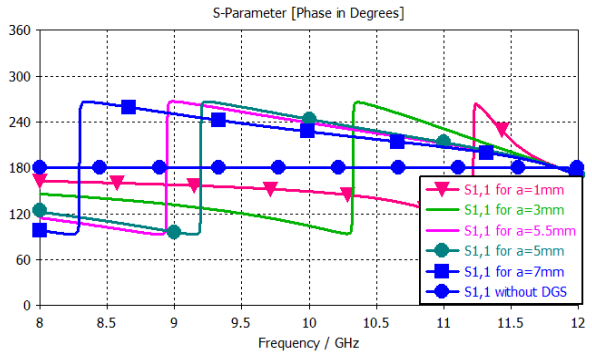

(b)

Figure-5. The parametric analysis of the length *a* of the DGS (a) reflection magnitude. (b) Reflection phase.

while when *a* = 7 mm, about resonance (8.25 GHz) the phase changes from 96° to 264°. The significant change in the reflection phase of the DGS at the resonant frequency demonstrates the potential of the DGS to be utilised as an alternative phase shifter and contributes to the beam steering ability in PAA. Therefore, the optimum dimension of *a* = 5 mm is selected for further investigation because the resonant of the DGS (9.1 GHz) is very close to the resonant frequency of the rectangular patches (9.08 GHz). This is to ensure that the significant change in the reflection phase of the DGS will provide considerable changes in the beam direction of the planar antenna arrays. However, the resonant frequency of the antenna arrays shifts 180 MHz downwards from 9.08 GHz to 8.9 GHz after insertion of DGS slot in the ground plane as demonstrated in Figure-4. The detail changes in the resonant frequency of the rectangular patches are tabulated in Table-2. Therefore, later analysis on the planar arrays with DGS slots is carried out at 9.0 GHz, which consider for both cases where the S_{11} is still below -10 dB.

Table-2. Change in the resonant frequency, *f* of the planar arrays for different length *a*.

a (mm)		*f* for 1st element	*f* for 2nd element
Without DGS		9.08	9.08
With DGS	1	8.94	8.93
	3	8.96	8.96
	5	8.90	8.91
	5.5	8.93	8.95
	7	9.01	9.01

In this work, it has been shown that the ability of the DGS to steer the main beam of the two rectangular patches. The same structure can employed in (Hajilou, 2012), (Ismaiel, 2014), (Xiao, 2011), (Jin, 2012), (Ahmed, 2012) for mutual coupling reduction. Therefore, the mutual interaction between the two elements is observed to be -3.5 dB for abbreviating is not discussed details in this paper.

Surface current distribution

Figure-6 shows the surface current distribution on the rectangular patches at 9 GHz when one patch antenna is excited while the second patch antenna is terminated with 50Ω load. Without DGS, the maximum surface current of 329.6 A/m occurs near to the edges of the rectangular patch while the middle part of the patch is very small. After insertion of the DGS (*a* = 5 mm), the maximum surface current reduces to 138.2 A/m where it flows near to the DGS slot.

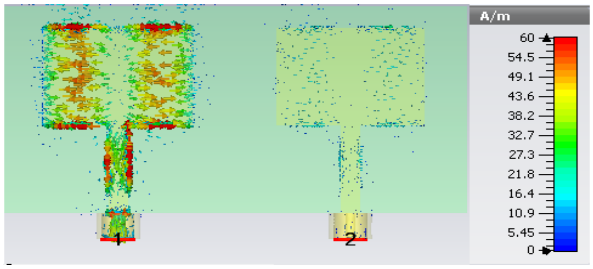

(a)

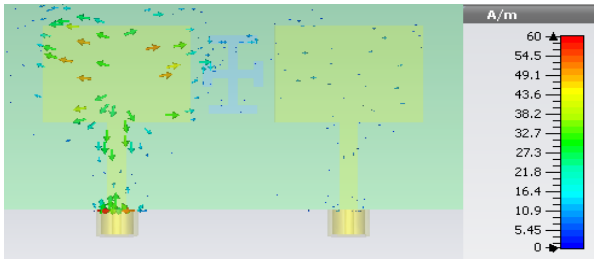

(b)

Figure-6. Snapshots surface current distribution on the ground plane at 9 GHz (a) without DGS (b) with DGS.

Beam steering performance

Table-3 summarises the directivity of the planar array, the angle of the main lobe and gain at the side lobe. Without DGS, the main beam is steering to 39° at 6.074 dB. The change to the direction of the main beam is relatively small when *a* = 1 mm because the DGS resonant frequency is far apart from rectangular patches' resonance as illustrated in Figure-7 (a). When *a* = 3 mm, the beam direction increases to 147°, however, the overall gain of the planar array reduces to 5.607 dB. When *a* = 5 mm, a significant change to the main beam direction is observed which is 137°, and the directivity of the gain relatively maintains at 6.06 dB. As described previously, the resonant of the DGS (9.1 GHz) is very close to the resonant frequency of the rectangular patches (9.08 GHz) therefore the significant change in the reflection phase of the DGS provides 98° change in the beam direction of the planar antenna arrays as illustrated in Figure-7(b). This demonstrates the best configuration of the planar arrays with DGS slot. The influence of the DGS slot is also visible in reducing the side lobes.

Table-3. Beam steering capability for different *a*.

a (mm)		Directivity D (dB_i)	Main lobe direction	Sidelobe (dB)
Without DGS		6.074	39°	-2.3
With DGS	1	6.320	47°	-1.9
	3	5.607	147°	-1.8
	5	6.056	137°	-3.1
	5.5	6.023	46°	-1.1
	7	6.141	43°	-1.8

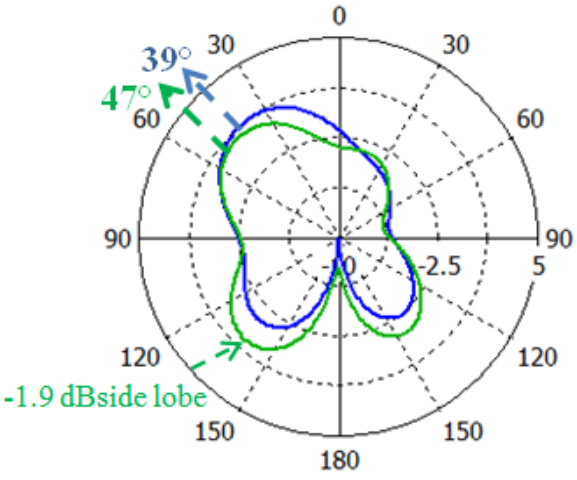

(a)

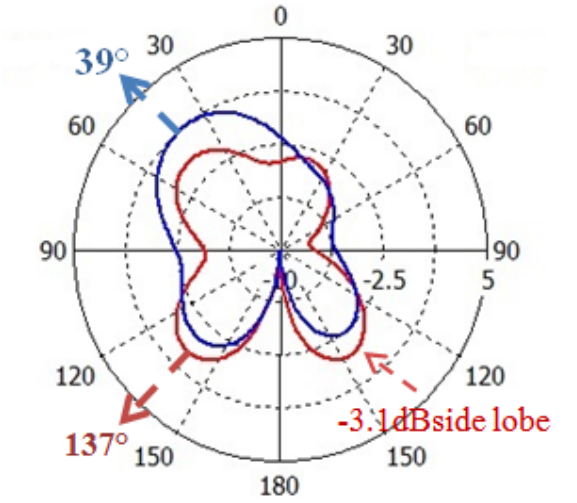

(b)

Figure-7. Radiation pattern, Plane $\theta=90^0$ and $\phi=270°$ at 9 GHz (a) without DGS and with DGS a = 1 mm (b) without DGS and with DGS a = 5 mm.

CONCLUSION

A design of 2×1 rectangular patches integrated with orthogonal-I-shaped DGS slot are presented. The work proposed demonstrate the ability to control a beam steering of the PAA at 9 GHz. The beam angle direction depends on the slot length a. The new array structure allows beam scanning from 39° without DGS to 137° with DGS a = 5 mm. The simulated results show a small reduction in the directivity gain due to a reduction of surface current which is influenced by the DGS, but this may be improved further by increasing the number of radiated elements.

REFERENCES

Ahmed M. I., Sebak A., Abdallah E. A., and Elhennawy H. 2012. Mutual coupling reduction using defected ground structure (DGS) for array applications. In proceedings of the 15th International Symposium on Antenna Technology and Applied Electromagnetics (ANTEM), pp. 1-4, Toulouse, France, June.

Alias H., Ali M. T., Ramli S. S. N., Sulaiman M. A., and Kayat S. 2013. A back lobe reduction of aperture coupled microstrip antenna using DGS. In: proceedings of the 10th International Conference on Electrical Engineering Electronics, Computer Telecommunications and Information Technology (ECTI-CON), pp. 1-5, Krabi, Thailand, May.

Armenta C. J. A., Porter S., and Marvin A. 2012. Reconfigurable phased array antennas with RF-MEMS on a PCB substrate. In proceedings of the Conference on Antennas and Propagation (LAPC), pp. 1-5, Loughborough, UK, November.

Balanis, C. A. 2005. Antenna Theory Analysis and Design. 3 rd ed., New York: John Wiley and Sons Inc.,

Bin Li, Hongbing Sun, and Weitao Lin. 2011. Signal-integrity simulation for beam steering system of phased array antennas. In: proceedings of the IEEE Conference on Electrical Design of Advanced Packaging and Systems Symposium (EDAPS), pp. 1-4, Hangzhou, China, December.

Can Ding, Guo Y. J., Pei-Yuan Qin, Bird T. S., and Yintang Yang. 2014. A defected microstrip structure (DMS)-based phase shifter and its application to beamforming antennas. IEEE Transaction on Antennas and Propagation, 62(2), pp. 641-651.

Can Ding, Guo Y. J., Pei-Yuan Qin, Bird T. S., and Yintang Yang. 2013. A novel phase shifter based on reconfigurable defected microstrip structure (RDMS) for beam-steering antennas. In: proceedings of the International Symposium on Antennas and Propagation (ISAP), pp. 993-996, Nanjing, China, October.

Chaozhu Zhang, Jing Zhang, and Lin Li. 2014. Triple band-notched UWB antenna based on SIR-DGS and fork-shaped stubs. Electronic Letters, 50(2), pp. 67-69.

Chirag G. and M. Kaur. 2014. A review of defected ground structure (DGS) in microwave design. International Journal of Innovative Research in Electrical, Electronics, Instrumentation and Control Engineering, 2(3), pp. 1-5, March.

Habashi A., Nourinia J., and Ghobadi C. 2012. A rectangular defected ground structure (DGS) for reduction of mutual coupling between closely-spaced microstrip antennas. In: proceedings of the 20th IEEE Conference on Electrical Engineering (ICEE), pp. 1347-1350, Tehran, Iran, May.

Haitao Liu, Gao S., and Tian Hong Loh. (2012). Low-cost beam-switching circularly-polarised antenna using tunable high impedance surface. In: proceedings of the Antennas and Propagation Conference (LAPC), pp. 1-3, Loughborough, UK, November.

Hajilou Y., Hassani H. R., and Rahmati B. 2012. Mutual coupling reduction between microstrip patch antennas. In: proceedings of the 6th European Conference on Antennas and Propagation (EUCAP), pp. 1-4, Prague, Czech Republic, March.

Ismaiel A. M. and Abdel-Rahman A. B. 2014. A meander shaped defected ground structure (DGS) for reduction of mutual coupling between microstrip antennas. In: proceedings of the 31st National Radio Science Conference (NRSC), pp. 21-26, Cairo, Egypt, April.

Jin Hua-song, Qiu Dong-dong, Rao Jia-ren, Zong Peng, and Becerra D. R. 2012. Application of EBG and DGS structure on antenna array. In: proceedings of the International Conference on Image Analysis and Signal Processing (IASP), pp. 1-4, Hangzhou, China, November.

John L. Volakis. 2007. Antenna Engineering Handbook. 4th ed., New York: McGraw and Hill.

Randy L. Haupt. 2010. Antenna Arrays a Computational Approach. New Jersey: John Wiley and Sons Inc.,

Shafaat Ali, A. K. M., Raza M., and Shah M.A. 2012. Design & development of a 32 elements X-band phased array antenna for airborne and space borne SAR payloads. In: proceedings of the 9th International Bhurban Conference on Applied Sciences and Technology (IBCAST), pp. 343-347. Islamabad, Pakistan, January.

Shikha, Chawla P., and Khanna R. 2013. Microstrip planar array antenna with improved DGS structure for multiband operation. In: proceedings of the International Conference on Signal Processing, Computing and Control (ISPCC), pp. 1-6. Solan, India, September.

Vikash K. and Sanjay Gurjar. 2013. A tutorial overview on the DGS to design microwave devices. In: proceedings of the National Conference on Trends in Signal Processing and Communication (TSPC'13), pp. 119-122, Muzaffarnagar, India, April.

Xiao, S., Tang, M.-C., Bai, Y.-Y., Gao, S., and Wang, B.-Z. 2011. Mutual coupling suppression in microstrip array using defected ground structure. IET Microwaves, Antennas and Propagation, vol. 5, no.12, pp. 1488-1494, May.